The measurement of the Interaction Matrices for the LINC-NIRVANA MCAO

Carmelo Arcidiacono[a,d], Maria Bergomi[b,d], Valentina Viotto[b,d], Luca Marafatto[b,d], Harald Baumeister[c], Thomas Bertram[c], Jürgen Berwein[c], Florian Briegel[c], Jacopo Farinato[b,d], Ralph Hofferbert[c], Frank Kittman[c], Martin Kürster[c], Kalyan Kumar Radhakrishnan Santhakumari[c], Tom Herbst[c], and Roberto Ragazzoni[b,d]

[a]INAF – Osservatorio Astronomico di Bologna, Via P. Gobetti 93/3, 40129 Bologna, Italy
[b]INAF – Osservatorio Astronomico di Padova, Vicolo dell'Osservatorio 5, 35127 Padova, Italy
[c]MPIA – Max-Plank-Institut für Astronomie, Königstuhl 17, 69117 Heidelberg, Germany
[d]ADONI – Laboratorio Nazionale di Ottica Adattiva, Italy

ABSTRACT

The commissioning of LINC-NIRVANA (LN) is ongoing at the Large Binocular Telescope (LBT). LN provides Multi-Conjugate Adaptive Optics (MCAO) correction for each side of the telescope using the Layer Oriented technique and using Natural Guide Stars (NGS). For each arm, two wavefront sensors (WFS), one conjugated to the ground and the other to 7km, co-add the light of all the reference stars within their respective fields of view, following the Multiple Field-of-View scheme. The two WFS separately control two deformable mirrors (DMs), the 672-actuator adaptive secondary of the LBT (ground layer) and a 349-actuator DM from Xinetics (7km layer). The DMs projections on the WFS cameras rotate, since the opto-mechanics of LN are pupil fixed, while the NGS rotate. We need to provide a distinct control matrix for approximately each degree of rotation. We succeed in obtaining valid control matrices through numerical interpolation of a few calibrated interaction matrices. In this paper, we present the daytime calibration strategy and procedures for LINC-NIRVANA's DM-WFS interaction matrices.

Keywords: Adaptive Optics, Multi-Conjugate Adaptive Optics, Calibration

1. INTRODUCTION

LINC NIRVANA[1] will realize the interferometric imaging focal station of the Large Binocular Telescope[2] (LBT). A double Layer Oriented[3–5] (LO) multi-conjugate adaptive optics[6,7] (MCAO) system assists the two arms of the interferometer,[8] supplying an high order wave-front correction. In particular, in LN we realize the Multiple Field of View[9,10] version of the LO, driving independent loops for the ground and the high layers correction respectively. According to the LO scheme we realize two independent loops using two independent Wavefront sensors (WFSs), collecting the light of up to 12 reference stars for the Ground WFS (GWS) and up to 8 for the high (HWS). We remark how the Field of View (Fov) of the two WFS are different: an 1arcmin to 3arcmin FoV radii annulus for the GWS and a full 1arcmin radius FoV for the HWS. The actual wavefront sensing device in each WFS is the Pyramid:[11] the light of all the natural reference stars in the FoV is split by as many optical prism (the pyramids) into four beams. Through a common objective, each beam generates a pupil image: the pupils corresponding to different references finally overlap on a WFS mimicking the geometrical overlap of footprint of the star beam in the atmosphere at the desired conjugation altitude: 0km and 7km for the GWS and HWS respectively. The deformable mirrors complete the conceptual design of the adaptive optics system, being the AdSec coupled to the GWS[12] and the 349-actuator DM from Xinetics mounted on the LN's bench for the HWS.[13]

LN sits on the rear, shared, bent Gregorian foci of the LBT: the LBT's M3 folding mirror forwards the light on a Field selector mirror on the LN the light from the Adaptive Secondary[14] (AdSec), see Figure 1. This system is implemented symmetrically on the two side of the LBT.

Further author information: (Send correspondence to C.A.)
C.A..: E-mail: carmelo.arcidiacono @ oabo.inaf.it, Telephone: +39 051 6357 316

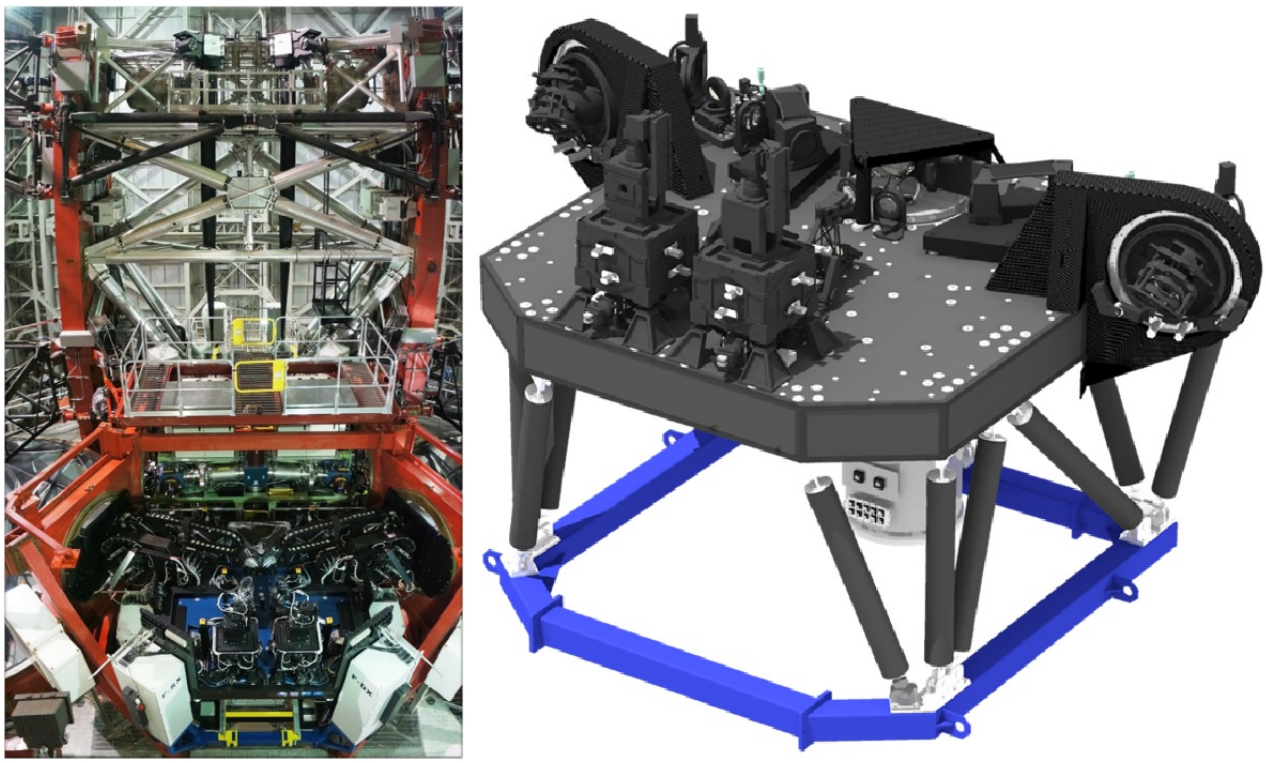

Figure 1. The picture shows the LN instrument mounted in the central platform of the LBT and a CAD sketch of the instrument hosting on the top part the AO WFS: HWSs are the two towers on the front and the GWSs are the ears on the left and right side. The infrared camera stands below the bench.

In order to counterbalance the field rotation, we implemented the mechanical derotation, for the two GWS, and the optical one, for the HWS sensors, to fix the positions of the focal planes with respect to the pyramids aboard each wavefront sensor. However, the derotation introduces the rotation of the pupil image on the wavefront sensors: the projection of the deformable mirrors on the sensor consequently changes. The proper rotation correction of the control matrix will be applied in real-time through the upload of a new numerically computed matrix. Here we present the procedure we followed for the calibration of the GWS interaction matrix we inverted to compute the control matrix.

We already discussed in a previous paper[15] of the error introduced by a not proper matching of the rotation angles of the WFS grid w.r.t. the actuator pattern on the DM and in[16] about the generation of the reconstructor matrix. Here we focus on the calibration procedure we follow to build the control matrix (reconstructor), that we need to upload it in the RTC to avoid the injection of WF error in the loops because of rotation of the DM-WFS mapping.

As of September 2016 the LN is being commissioned[17] at the LBT observatory.

2. MAIN COMPONENTS

The calibration procedure of the HWS and GWS are conceptually identical and, for the sake of space, we limit the calibration description to the GWS channel only.

The LN's GWS is a multi-pyramid WFS coupled to the AdSec of the LBT. Following the Layer Oriented scheme the light of all the reference stars, once split by the corresponding refractive pyramid, is imaged on a single detector (CCD50) properly focused on the pupil plane (the AdSec is the pupil of the telescope). Each pyramid is mounted at the end of an optical relay (star enlarger) moving the F/ from 15 to 187.5 in order to project a pupil image diameter of 48px on the 128×128px CCD50, see Figure 3 and Figure 4.

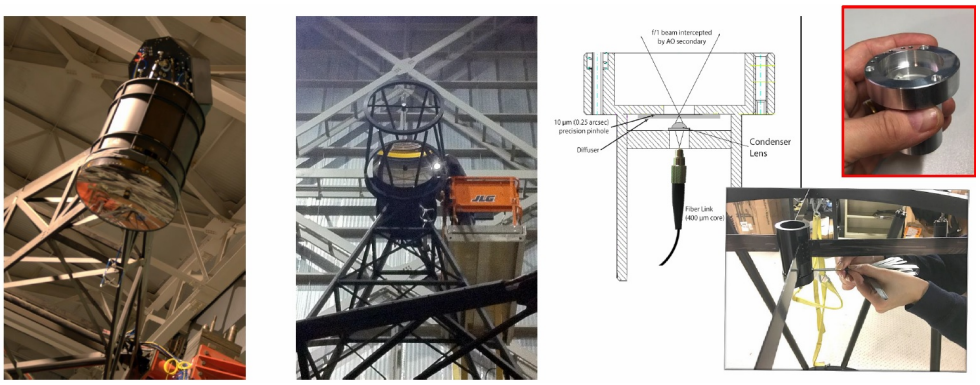

Figure 2. From left to right: the Adaptive Secondary (AdSec) of the LBT; the Retro-Reflector mounted on the AdSec; the light source: a fiber mounted on the focus of the AdSec.

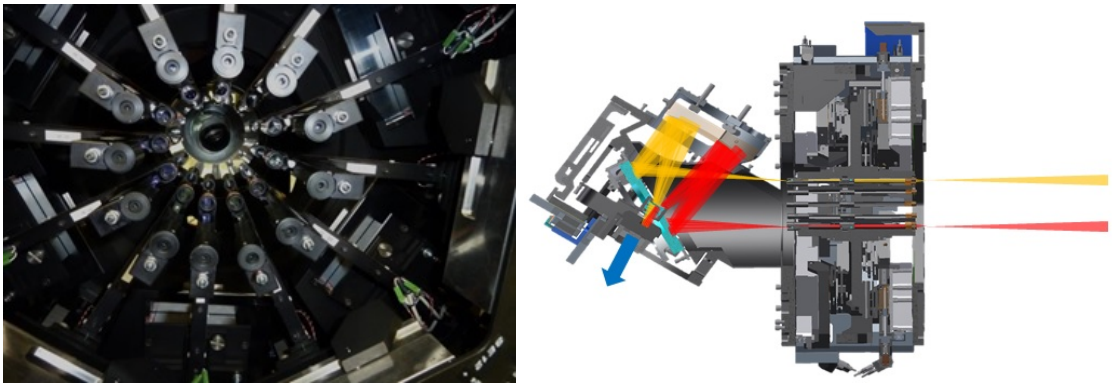

Figure 3. On the left the 12 pyramids, each one being hosted on board of a star enlarger, on the right a cross section of the GWS sensor with enhanced the optical path of two reference stars. The light entering from the right side is forwarded to the pyramids placed in the focal plane.

We have the chance to perform daytime calibrations using a fiber source placed mechanically on the focus of the AdSec, see Figure 2, saving in this way precious night time for commissioning activities.

The fiber is mounted trough on the retro-reflector unit, originally designed to perform the calibration of the LBTI and FLAO WFS calibrations.[18] This was reversibly modified to host our light source. Actually, after our modification the name retro-reflector may be misleading since we placed a fiber holder instead of the original optical system composed by a F/1 parabola and a flat mirror.

Each system pyramid+star enlarger is mounted on a couple of linear stages that allow the patrolling of the WFS FoV. The optical system of each pyramid unit is required to produce images of the pupil with an error on the diameter less than 1/10 of sub-aperture (1subap = $48\mu m$ in our case with bin2). Let us remind that a pixel on the detector corresponds to a sub-aperture on the LO-pyramid WFS. Given the small wavefront error[19] (WFE) introduced by the optical relay in front of the pyramid we may measure almost identical WFS-Deformable Mirror Interaction Matrix for all the pyramids.

3. INSTRUMENTAL SETUP

Being the interaction Matrix (IM) of the different pyramids interchangeable, we measured it on only one. We illuminated the pyramid projecting an \F/1 beam on the AdSec shell and placed a fiber assisted optical system on one focus of the concave elliptical mirror (the AdSec) and simulated the effect of a partially corrected (it's not diffraction limited) focal plane star by a couple diffuser/pin-hole generating a disk uniformly illuminated of \0.5 arcsec on the pyramid pin. Special attention was taken to generate a uniform illumination of the mirror shell in

order to not inject errors in the IM measurement process, since we want to simulate the light from a real star, that will produce a uniformly illuminated pupil image. The CCD binning for the foreseen night-time operations is set to two, making 64×64 the size of the images on which we measure the four pupil differential illumination. Using binning two the slopes are measured on 24px diameter pupils and a subaperture has a side of $48\mu n$.

Both GWS and HWS CCDs are mounted on a couple of linear stages[20] positioned one on top of the other in a 90 degrees configuration. The stages are remotely controlled allowing an active centering of the detector with respect to the metapupil image.

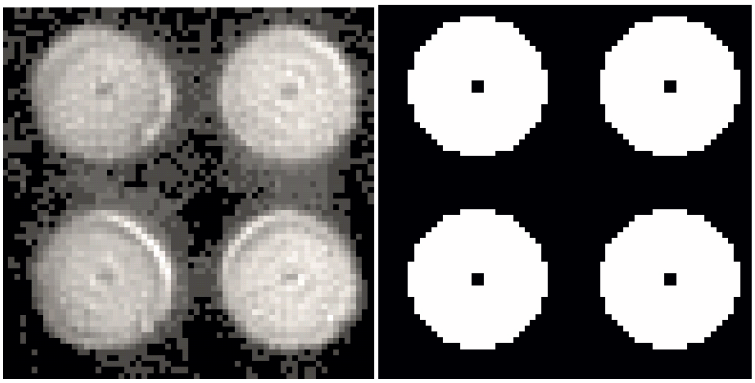

Figure 4. On the left, a frame from the the CCD50 on the GWS WFS looking on a single fiber with AdSec applying the flat shape. On the right: the pupil mask as encoded in the Real Time Computer (RTC) software. Here the system used a 2×2 binning on chip, the same used for on sky operations in the case of bright reference stars.

4. MEASUREMENTS PREPARATION

In order to start with the measurements of the IM, we needed to properly center the pupil images with respect to the mask used by the RTC for selecting the valid sub-aperture from the CCD images. Since we need to perform rotation of the IM matrix to take into account for optical rotation of AdSec with respect to the detector, we needed to identify the center of rotation of the mirror images on the CCD and moving it as close as possible to the center of the circular pupil we draw for the RTC mask. This was an iterative process in which we use as reference the signal of the first 100 modes of the Karhunen-Loeve (KL) modal base used to control the mirror for different position of the CCD50 linear stages. In this way, and independently on the optical illumination of the pupil, we succeeded to perform a centering. In a later stage, as part of the acquisition procedure, we will need to center the pupil image with respect to the four pupil image geometry obtained by looking into the mirror modes shape. We perform this later centering with a precision of 1/10 of sub-aperture.

From the operational point of view, we built a python script that takes care of the measurements by preparing the KL modes (the M2C, modes to command, matrix), defining the push-pull history file to be uploaded to the AdSec Basic Computation Unit (BCU) on board of the AdSec.[21] The script interacts with the AdSec in order to finally download the measured slopes history file corresponding to the applied shapes. The script takes care of the slopes measurement extraction and of the generation of a IM sample corresponding to about 12-16 repetitions of the push-pull sequence for each mode. Finally the script averages the IMs generated in this way and finally compute the average one.

5. IM CALIBRATIONS

The calibration process requires the pyramid working around the linear regime. For the IM measurements we needed to follow an iterative process in order to achieve this goal. For the initial measurements we needed to save IM with 2,5,10, 20, 50, 70, 90 and 100 modes and as many reconstructors in order to build a well performing optical flat of the deformable mirror. This fine tuning process is needed at the very beginning of the calibration procedure only.

Once this best shape was achieved, we save this shape as reference flat of the DM. Later, as part of the calibration measurement, we perform a minor revision of the flat, adjusting the AdSec command vector by closing an AO loop with 50 modes and saving the average mirror shape that we will use for the following steps as new DM-flat.

For each calibration run we save a set of IMs for 2, 50 and 100modes.

6. DIFFERENT ANGLES

As said in the introduction, LINC-NIRVANA WFSs needs to follow sky rotation to keep the pyramids properly centered on the reference stars focal plane images. This generates the rotation of the pupil on the detector that actually sees the rotation of both the actuators map and the slopes directions.

Since the Influence Function of the single actuator is not properly sampled using 24 sub-aperture across the pupil (we have 28 actuators along the diameter) we suffer of under-sampling. Because of this some couple of actuators fall inside one sub-aperture making the WFS insensitive to possible slopes between the two.

One of the challenges is that the sensitivity of the WFS to this feature change with the rotation.

To recover a better resolution and having in mind as goal to compute the average sensitivity on all the actuators, we need to perform more measurements for different positions of the actuator pattern w.r.t. the grid of sub-apertures on the detector. Because of geometrical reasons (the actuator pattern is made of rings) and since the challenge we want to deal is produced by the pupil rotation we choose to derotate instead of, for example, moving in X and Y the detector in the WFS. We measured 5 different interaction matrices for as many rotation angles. In this way we measured the effect of each actuator: we performed rotation steps not equally angularly spaced and covering 10degree of rotation taking advantage of the periodicity of the actuators pattern.

Because of the noise induced by vibrations we needed to perform separately the tip-tilt measurements averaging \50 times more push-pulls couples than what we did for the other modes. For each angle we saved a 50modes IM and we used this to adjust the flat of the AdSec to finally measures the 100modes IM. Once we have the 5 interaction matrices we counter-rotates them rotating the map of the X and Y slopes and then rotating slopes vector both of the corresponding angle to match the angle zero for the rotation. We then average them and this mean IM is rotated back to the various angle.

Our on-sky strategy foresees to update the reconstructor matrix (100modes) for every 1degree of rotation in order to do not affect the performance. The angle zero IM is then rotated for angles between -60 and 60 degrees.

The computation of the matrices is performed off-line and the full set of possible angles is stored on the LN servers. During operation the RTC system is started having loaded the first two reconstructor expected. The matrix vector multiplication of the control matrix by the slope vector is performed on the BCU[22] on board of the AdSec.

7. DIFFERENCE WITH THE HWS

The calibration procedure for the HWS is very similar, with a few exception: since the AdSec is not needed we performed the calibration using our internal calibration unit. On the unit we have the possibility to install 8 fiber simultaneously covering the full metapupil. Let us remark that using one single fiber in the case of the HWS is not producing the desired measurements since the metapupil is only partially filled. On the other side, we have the possibility to turn on all the fibers simultaneously making the IM measurements possible. In the case of the HWS the rotation of the pupil is not directly affecting the measurements since the controlled DM is the internal one. However it is clocked with the pupil making all the description made for the GWS valid also for the HWS.

8. CONCLUSIONS

We described the calibration strategy for the GWS (and HWS) of the LINC-NIRVANA. The complication of the rotation of the DM as seen by the WFS was solved by averaging different interaction matrix recorded at different angles. The interaction matrix computed in this way were successfully used both in the laboratory and on sky[23] and both for the GWS and HWS.

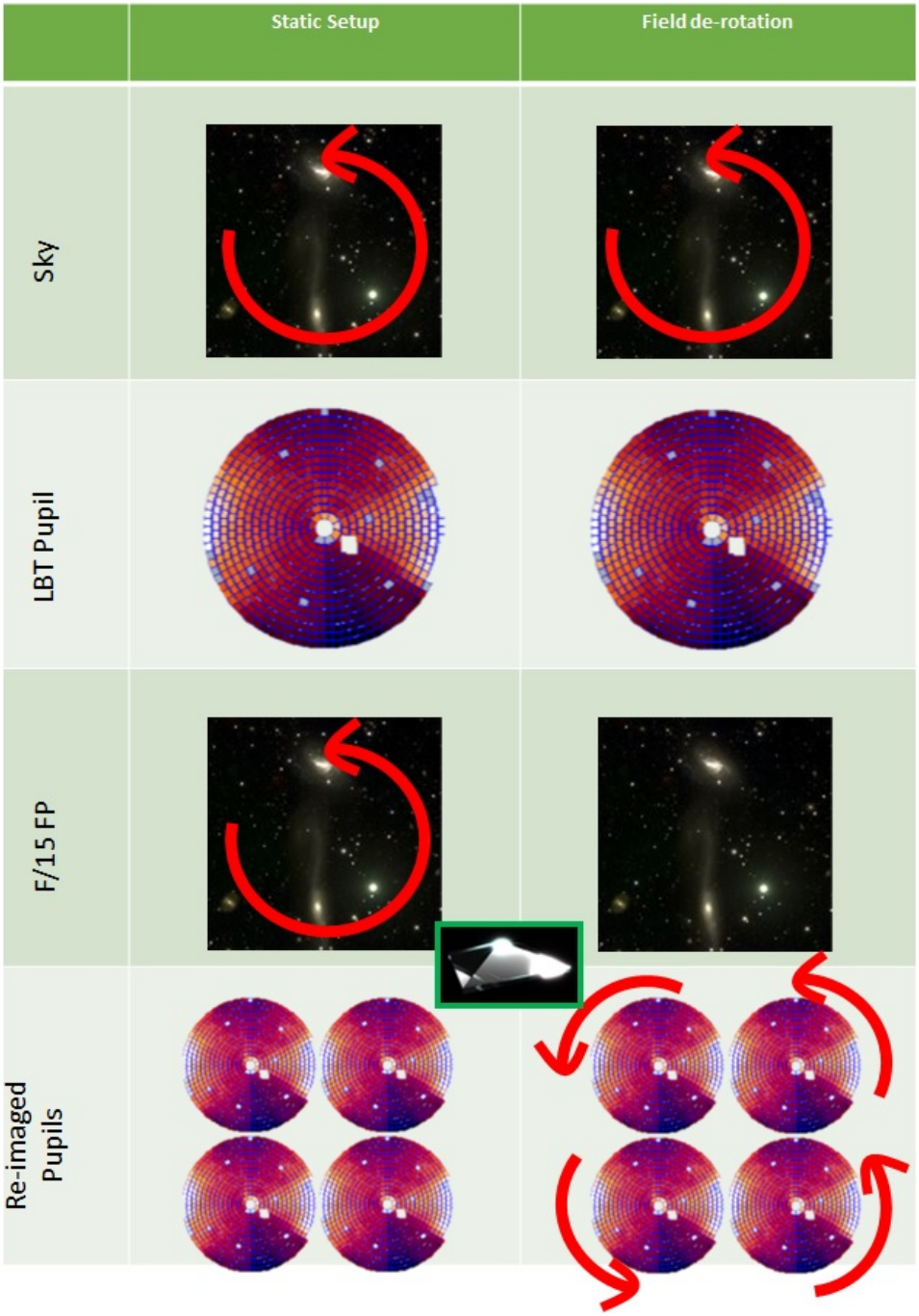

Figure 5. On the left column the effect of the sky rotation in static condition leaving the bearing offline. On the right the bearing follows sky rotation but in this way produce the rotation of the pupil as seen from the WFSs.

ACKNOWLEDGMENTS

The authors wish to thank the LBTO and in particular the LBT crew that supported all our activities at the telescope.

REFERENCES

[1] Ragazzoni, R., Herbst, T. M., Gaessler, W., Andersen, D., Arcidiacono, C., Baruffolo, A., Baumeister, H., Bizenberger, P., Diolaiti, E., Esposito, S., Farinato, J., Rix, H. W., Rohloff, R.-R., Riccardi, A., Salinari, P., Soci, R., Vernet-Viard, E., and Xu, W., "A visible MCAO channel for NIRVANA at the LBT," in [*Adaptive Optical System Technologies II*], Wizinowich, P. L. and Bonaccini, D., eds., *Proc. SPIE* **4839**, 536–543 (2003).

[2] Hill, J. M., "The Large Binocular Telescope," *Applied Optics* **49**, 115–122 (Apr. 2010).

[3] Ragazzoni, R., "Adaptive optics for giant telescopes: NGS vs. LGS," in [*Proceedings of the Backaskog workshop on extremely large telescopes*], Andersen, T., Ardeberg, A., and Gilmozzi, R., eds., 175–180 (2000).

[4] Ragazzoni, R., Farinato, J., and Marchetti, E., "Adaptive optics for 100-m-class telescopes: new challenges require new solutions," in [*Adaptive Optical Systems Technology*], Wizinowich, P. L., ed., *Proc. SPIE* **4007**, 1076–1087 (2000).

[5] Arcidiacono, C., Lombini, M., Farinato, J., and Ragazzoni, R., "Toward the first light of the Layer Oriented Wavefront Sensor for MAD.," *Memorie della Societa Astronomica Italiana* **78**, 708–711 (2007).

[6] Beckers, J. M., "Increasing the size of the isoplanatic patch with multiconjugate adaptive optics.," in [*ESO Conference on Very Large Telescopes and their Instrumentation*], **2**, 693–703 (1988).

[7] Beckers, J. M., "Detailed compensation of atmospheric seeing using multiconjugate adaptive optics.," in [*Active Telescope Systems*], *Proc. SPIE* **1114**, 215–217 (1989).

[8] Viotto, V., Ragazzoni, R., Arcidiacono, C., Bergomi, M., Brunelli, A., Dima, M., Farinato, J., Gentile, G., Magrin, D., Cosentino, G., Diolaiti, E., Foppiani, I., Lombini, M., Schreiber, L., Bertram, T., Bizenberger, P., De Bonis, F., Gässler, W., Herbst, T., Kuerster, M., Meschke, D., Mohr, L., and Rohloff, R.-R., "A very wide field wavefront sensor for a very narrow field interferometer," in [*Optical and Infrared Interferometry II*], *Proc. SPIE* **7734**, 77343M (July 2010).

[9] Ragazzoni, R., Diolaiti, E., Farinato, J., Fedrigo, E., Marchetti, E., Tordi, M., and Kirkman, D., "Multiple field of view layer-oriented adaptive optics. Nearly whole sky coverage on 8 m class telescopes and beyond," *Astron. Astrophys.* **396**, 731–744 (2002).

[10] Farinato, J., Ragazzoni, R., Arcidiacono, C., Brunelli, A., Dima, M., Gentile, G., Viotto, V., Diolaiti, E., Foppiani, I., Lombini, M., Schreiber, L., Bizenberger, P., De Bonis, F., Egner, S., Gässler, W., Herbst, T., Kürster, M., Mohr, L., and Rohloff, R., "The Multiple Field of View Layer Oriented wavefront sensing system of LINC-NIRVANA: two arcminutes of corrected field using solely Natural Guide Stars," in [*Adaptive Optics Systems*], *Proc. SPIE* **7015** (2008).

[11] Ragazzoni, R., "Pupil plane wavefront sensing with an oscillating prism," *Journal of Modern Optics* **43**, 289–293 (1996).

[12] Conrad, A. R., Arcidiacono, C., Baumeister, H., Bergomi, M., Bertram, T., Berwein, J., Biddick, C., Bizenberger, P., Brangier, M., Briegel, F., Brunelli, A., Brynnel, J., Busoni, L., Cushing, N., De Bonis, F., De La Pena, M., Esposito, S., Farinato, J., Fini, L., Green, R. F., Herbst, T., Hofferbert, R., Kittmann, F., Kuerster, M., Laun, W., Meschke, D., Mohr, L., Pavlov, A., Pott, J.-U., Puglisi, A., Ragazzoni, R., Rakich, A., Rohloff, R.-R., Trowitzsch, J., Viotto, V., and Zhang, X., "LINC-NIRVANA Pathfinder: testing the next generation of wave front sensors at LBT," in [*Adaptive Optics Systems III*], *Proc. SPIE* **8447**, 84470V (2012).

[13] Zhang, X., Gaessler, W., Conrad, A. R., Bertram, T., Arcidiacono, C., Herbst, T. M., Kuerster, M., Bizenberger, P., Meschke, D., Rix, H.-W., Rao, C., Mohr, L., Briegel, F., Kittmann, F., Berwein, J., Trowitzsch, J., Schreiber, L., Ragazzoni, R., and Diolaiti, E., "First laboratory results with the LINC-NIRVANA high layer wavefront sensor," *Optics Express* **19**, 16087–16095 (Aug. 2011).

[14] Riccardi, A., Brusa, G., Salinari, P., Gallieni, D., Biasi, R., Andrighettoni, M., and Martin, H. M., "Adaptive secondary mirrors for the Large Binocular Telescope," *Proceedings of SPIE* **4839**, 721–732 (2003).

[15] Arcidiacono, C., Bertram, T., Ragazzoni, R., Farinato, J., Esposito, S., Riccardi, A., Pinna, E., Puglisi, A., Fini, L., Xompero, M., Busoni, L., Quiros-Pacheco, F., and Briguglio, R., "Numerical control matrix rotation for the LINC-NIRVANA multiconjugate adaptive optics system," in [*Adaptive Optics Systems II*], *Proc. SPIE* **7736**, 77364J (July 2010).

[16] Bertram, T., Kumar Radhakrishnan Santhakumari, K., Marafatto, L., Arcidiacono, C., Berwein, J., Ragazzoni, R., and Herbst, T. M., "Wavefront sensing in a partially illuminated, rotating pupil," in [*Adaptive Optics Systems IV*], *Proc. SPIE* **9148**, 91485M (Aug. 2014).

[17] Herbst, T. M., Arcidiacono, C., Bertram, T., Bizenberger, P., Briegel, F., Hofferbert, R., Kürster, M., and Ragazzoni, R., "MCAO with LINC-NIRVANA at LBT: preparing for first light," in [*Adaptive Optics Systems V*], *Proc. SPIE* **9909**, 99092U (July 2016).

[18] Esposito, S., Riccardi, A., Quirós-Pacheco, F., Pinna, E., Puglisi, A., Xompero, M., Briguglio, R., Busoni, L., Fini, L., Stefanini, P., Brusa, G., Tozzi, A., Ranfagni, P., Pieralli, F., Guerra, J. C., Arcidiacono, C., and Salinari, P., "Laboratory characterization and performance of the high-order adaptive optics system for the Large Binocular Telescope," *Applied Optics* **49**, G174+ (Nov. 2010).

[19] Marafatto, L., Bergomi, M., Brunelli, A., Dima, M., Farinato, J., Farisato, G., Lessio, L., Magrin, D., Ragazzoni, R., Viotto, V., Bertram, T., Bizenberger, P., Brangier, M., Briegel, F., Conrad, A., De Bonis, F., Herbst, T., Hofferbert, R., Kittmann, F., Kürster, M., Meschke, D., Mohr, L., and Rohloff, R.-R., "Aligning a more than 100 degrees of freedom wavefront sensor," in [*Adaptive Optics Systems III*], *Proc. SPIE* **8447**, 84476F (July 2012).

[20] Soci, R., Ragazzoni, R., Herbst, T. M., Farinato, J., Gaessler, W., Baumeister, H., Rohloff, R.-R., Diolaiti, E., Xu, W., Andersen, D. R., Egner, S. E., Arcidiacono, C., Lombini, M., Ebert, M., Boehm, A., Muench, N., and Xompero, M., "LINC-NIRVANA: mechanical challanges of the MCAO wavefront sensor," in [*Advancements in Adaptive Optics.*], Bonaccini Calia, D., Ellerbroek, B. L., and Ragazzoni, R., eds., *Proc. SPIE* **5490**, 1286–1295 (2004).

[21] Biasi, R., Andrighettoni, M., Veronese, D., Biliotti, V., Fini, L., Riccardi, A., Mantegazza, P., and Gallieni, D., "LBT adaptive secondary electronics," in [*Adaptive Optical System Technologies II*], Wizinowich, P. L. and Bonaccini, D., eds., *Proc. SPIE* **4839**, 772–782 (Feb. 2003).

[22] Berwein, J., Bertram, T., Conrad, A., Briegel, F., Kittmann, F., Zhang, X., and Mohr, L., "End-To-End performance test of the LINC-NIRVANA Wavefront-Sensor system.," in [*Second International Conference on Adaptive Optics for Extremely Large Telescopes. Online at ¡A href="http://ao4elt2.lesia.obspm.fr"¿http://ao4elt2.lesia.obspm.fr¡/A¿, id.P44*], P44 (Sept. 2011).

[23] Bergomi, M., Viotto, V., Arcidiacono, C., Marafatto, L., Farinato, J., Baumeister, H., Bertram, T., Berwein, J., Briegel, F., Conrad, A., Kittman, F., Kopon, D., Hofferbert, R., Magrin, D., Radhakrishnan Santhakumari, K. K., Puglisi, A., Xompero, M., Briguglio, R., Quiros-Pacheco, F., Herbst, T. M., and Ragazzoni, R., "First light of the LINC-NIRVANA Pathfinder experiment," in [*Adaptive Optics Systems IV*], *Proc. SPIE* **9148**, 91482Y (July 2014).